25 Gbit/s QPSK Hybrid Fiber-Wireless Transmission in the W-Band (75–110 GHz) With Remote Antenna Unit for In-Building Wireless Networks

Xiaodan Pang, Student Member, IEEE
Antonio Caballero
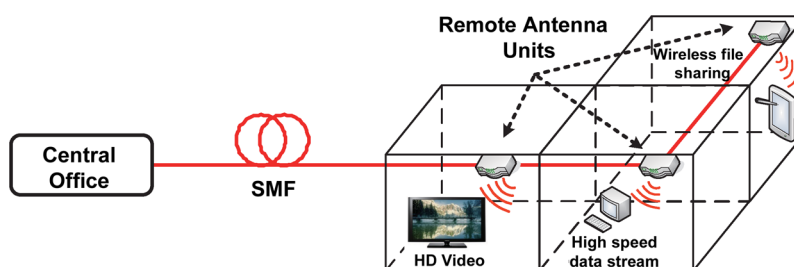**Anton Dogadaev**
Valeria Arlunno
Lei Deng
Robert Borkowski
Jesper S. Pedersen
Darko Zibar, Member, IEEE
Xianbin Yu, Member, IEEE
Idelfonso Tafur Monroy, Member, IEEE

25 Gbit/s QPSK Hybrid Fiber-Wireless Transmission in the W-Band (75–110 GHz) With Remote Antenna Unit for In-Building Wireless Networks

Xiaodan Pang,[1] *Student Member, IEEE*, **Antonio Caballero,**[1] **Anton Dogadaev,**[1] **Valeria Arlunno,**[1] **Lei Deng,**[2] **Robert Borkowski,**[1] **Jesper S. Pedersen,**[1] **Darko Zibar,**[1] *Member, IEEE*, **Xianbin Yu,**[1] *Member, IEEE*, **and Idelfonso Tafur Monroy,**[1] *Member, IEEE*

[1]DTU Fotonik, Department of Photonics Engineering, Technical University of Denmark, 2800 Kgs. Lyngby, Denmark
[2]School of Optoelectronics Science and Engineering, HuaZhong University of Science and Technology, Wuhan 430074, China

Abstract: In this paper, we demonstrate a photonic up-converted 25 Gbit/s fiber-wireless quadrature phase shift-keying (QPSK) data transmission link at the W-band (75–110 GHz). By launching two free-running lasers spaced at 87.5 GHz into a standard single-mode fiber (SSMF) at the central office, a W-band radio-over-fiber (RoF) signal is generated and distributed to the remote antenna unit (RAU). One laser carries 12.5 Gbaud optical baseband QPSK data, and the other acts as a carrier frequency generating laser. The two signals are heterodyne mixed at a photodetector in the RAU, and the baseband QPSK signal is transparently up-converted to the W-band. After the wireless transmission, the received signal is first down-converted to an intermediate frequency (IF) at 13.5 GHz at an electrical balanced mixer before being sampled and converted to the digital domain. A digital-signal-processing (DSP)-based receiver is employed for offline digital down-conversion and signal demodulation. We successfully demonstrate a 25 Gbit/s QPSK wireless data transmission link over a 22.8 km SSMF plus up to 2.13 m air distance with a bit-error-rate performance below the 2×10^{-3} forward error correction (FEC) limit. The proposed system may have the potential for the integration of the in-building wireless networks with the fiber access networks, e.g., fiber-to-the-building (FTTB).

Index Terms: Microwave photonics, radio over fiber, optical communications.

1. Introduction

The emergence of mobile devices such as multifunction mobile phones and tablets accompanied with future bandwidth intensive applications, e.g., 3-D Internet and Hi-Vision/Ultra High Definition TV data (more than 24 Gbit/s) [1], has become one of the drivers for demanding wireless data capacity on the scale of tens of gigabits per second. It is highly desirable that the future wireless links will possess the same capacity with the optical fibers to realize the seamless hybrid fiber-wireless access over the last mile [2]. Radio-over-fiber (RoF) communication systems are considered to be one of the most promising candidates to provide ultrabroadband services while maintaining high mobility in this
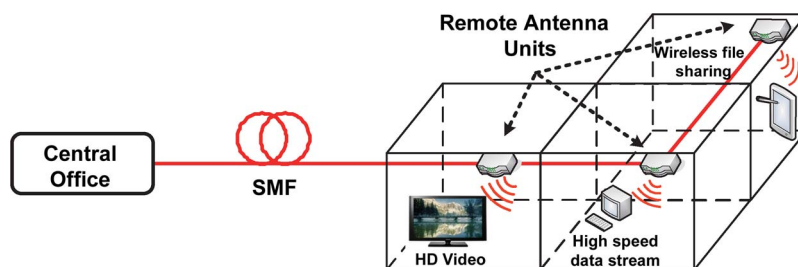
Fig. 1. Hybrid fiber-wireless access system for multiapplications in-building environment.

context. As shown in Fig. 1, an in-building hybrid fiber-wireless access system implemented via RoF technology provides an elegant solution for flexible multiservice wireless access. A key point in such scenario is that the remote antenna units (RAUs) should keep a simple, passive and compact structure, leading to a low-cost implementation [3], [4].

Meanwhile, there are mainly two approaches to achieve tens of gigabits per second wireless capacity. One possible solution is to increase the wireless spectral efficiency to enlarge the data throughput over the same bandwidth [5]. However, it will largely increase the signal-to-noise ratio (SNR) requirement, as well as the receiver complexity. Another straightforward solution is to raise the carrier frequency to higher frequency bands, e.g., millimeter-wave (MMW) range (30–300 GHz), where a broader bandwidth is available. Currently, the frequency bands below 100 GHz have limited unlicensed bandwidth left for wireless transmission [6]. In recent years, a number of multigigabit hybrid fiber-wireless links operating at the 60 GHz band are investigated and reported [5], [7], [8]. Nevertheless, the under-exploited higher frequency range at 100 GHz and above is becoming a timely relevant research topic for its wider bandwidth availability.

Recently, the W-band (75–110 GHz) is attracting increasing attention due to its potential to provide the requested high capacity [6]. The Federal Communications Commission (FCC) has opened the commercial use of spectra in the 71–75.5 GHz, 81–86 GHz, 92–100 GHz, and 102–109.5 GHz bands [9], which are recommended for high-speed wireless communications. Analysis and measurements on W-band signal generation, detection, and wireless transmission properties are under intensive investigation. In terms of signal generation and detection scheme, W-band channel properties measurements and signal transmissions based on electronically frequency up and down-conversion are reported in [10]–[12], while an up to 40 Gbit/s wireless signal transmission in the W-band using both photonic generation and detection without air transmission is demonstrated and detailed analyzed [13], [14]. Specifically, an ultrabroadband photonic down-converter based on optical comb generation that can operate from microwave up to 100 GHz has recently been introduced [15]. Considering the wireless distance, data rate, and signal formats transmitted in the W-band, to date, 10 Gbit/s transmission over 400 m single-mode fiber (SMF) plus 120 m wireless distance with simple amplitude shift-keying (ASK) modulation is reported [16], while an error-free (1×10^{-12}) 20 Gbit/s on–off-keying (OOK) signal transmission through 25 km SMF and 20 cm wireless is demonstrated [17]. To achieve higher spectral efficiency, quadrature phase shift-keying (QPSK) and 16-quadrature amplitude modulation (16-QAM) have also been used to obtain 20 Gbit/s [18] and 40 Gbit/s [19] in the W-band. In [18] and [19], a coherent optical heterodyning method is used to generate the W-band wireless carrier, and transmission performance below forward error correction (FEC) limit of 2×10^{-3} is achieved with 30 mm wireless distance. By using an optical frequency comb generator, a three-channel 8.3 Gbit/s/ch optical orthogonal frequency-division-multiplexing (OOFDM) transmission over 22.8 km SMF with up to 2 m air distance is reported in [20]. More recently, an up to 100 Gbit/s line rate wireless transmission in the W-band with air distance of 1.2 m by combining optical polarization multiplexing and wireless spatial multiplexing has been demonstrated; however, there are only a few meters of fiber transmission [21]. Nevertheless, considering the integration of the in-building wireless networks with the existing optical fiber access networks, e.g., fiber-to-the-building (FTTB) networks, a system with a better compromise between fiber transmission distance, wireless coverage, and data rate need to be further developed.
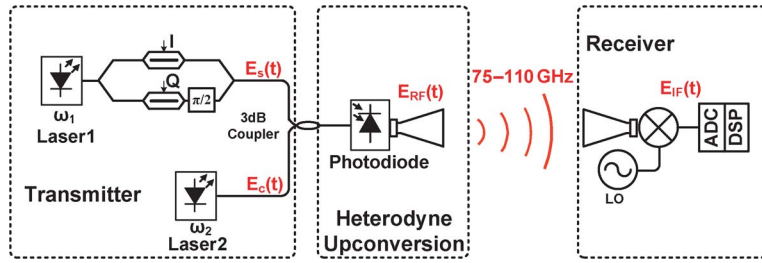
Fig. 2. Block diagram of hybrid optical fiber-wireless system using incoherent heterodyne up-conversion and electrical and digital down-conversion.

In this paper, we propose and experimentally demonstrate a hybrid fiber-wireless link at the W-band which can be potentially used for integrating the in-building wireless access networks with the optical fiber access networks, as shown in Fig. 1. By using photonic up-conversion technique with two free-running laser heterodyning (incoherent method), the proposed system seamlessly converts an optical baseband signal into the W-band. For demonstration, a 25 Gbit/s QPSK signal occupying a bandwidth of 25 GHz centered at 87.5 GHz is transmitted. A W-band low-noise amplifier (LNA) and a broadband balanced mixer are employed at the receiver for down-converting the received signal to an intermediate frequency (IF) centering at 13.5 GHz, and a digital-signal-processing (DSP)-based signal demodulator is implemented for digital down-conversion, I/Q separation, synchronization, equalization, and signal demodulation. The data transmitted after 22.8 km SMF plus 2.3 m wireless are successfully recovered with a bit-rate-ratio (BER) performance well below the FEC limit of 2×10^{-3}. The RAU in this proposed downlink system consists of only a fast responsive photodetector and a W-band horn antenna, therefore fulfilling the passive, simplicity, and low-cost requirements. When considering the bidirectional transmission, an electrical local oscillator (LO) may also be needed in the RAU for a low-cost optical modulation in the uplink.

2. Principle of Incoherent Heterodyne Up-Conversion and Two Stage Down-Conversion

Fig. 2 shows the block diagram of the proposed system. The W-band signal is generated by heterodyning mixing the baseband optical signal with a second free-running lightwave at the photodetector. At the receiver, the W-band signal is first down-converted electrically to an IF and then sampled and digitally converted down to the baseband.

At the transmitter, the inphase and quadrature branches of the I/Q modulator are, respectively modulated by two binary data sequences $I(t)$ and $Q(t)$. The baseband optical QPSK signal $\hat{E}_s(t)$ and the carrier frequency generating laser $\hat{E}_c(t)$ can be represented as

$$\hat{E}_s(t) = \sqrt{P_s} \cdot [I(t) + jQ(t)] \cdot e^{[-j(\omega_s t + \phi_s(t))]} \cdot \hat{e}_s \tag{1}$$

$$\hat{E}_c(t) = \sqrt{P_c} \cdot e^{[-j(\omega_c t + \phi_c(t))]} \cdot \hat{e}_c \tag{2}$$

where P_s, ω_s, and $\phi_s(t)$ represent the optical power, angular frequency, and phase of the signal laser, respectively, and P_c, ω_c and $\phi_c(t)$ represent the carrier generating laser. $\hat{e}_s$ and $\hat{e}_c$ are the optical polarization unit vectors. The combined signal is beating at a photodiode for heterodyne up-conversion, and the output signal $E_{out}(t)$ can be described as

$$E_{out}(t) \propto |E_s(t) + jE_c(t)|^2 = P_s + P_c + E_{RF}(t)$$
$$E_{RF}(t) = 2\sqrt{P_s P_c} \cdot [I(t) \cdot \sin(\triangle\omega t + \triangle\phi(t)) + Q(t) \cdot \cos(\triangle\omega t + \triangle\phi(t))] \cdot \hat{e}_s\hat{e}_c$$
$$\triangle\omega = \omega_c - \omega_s, \quad \triangle\phi(t) = \phi_c(t) - \phi_s(t) \tag{3}$$

where $E_{RF}(t)$ represents the generated RF signal transmitted into the air with carrier frequency of $\triangle\omega$. At the receiver, an electrical sinusoidal LO signal is mixed with the received RF signal at a
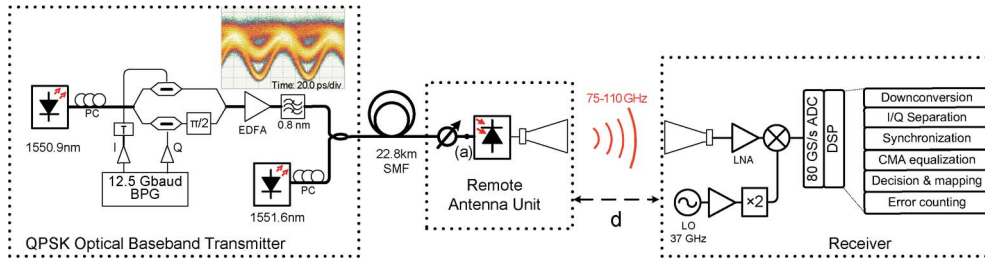
Fig. 3. Experimental setup for hybrid fiber-wireless transmission of 25 Gbit/s QPSK signals in the W-band.
BPG: Binary pattern generator. (The eye diagram of the QPSK baseband signal is shown in the inset.)

balanced mixer. The LO signal with power P_{LO}, angular frequency ω_{LO}, and phase $\phi_{LO}(t)$ is expressed as $E_{LO}(t) = \sqrt{P_{LO}} \cdot \cos(\omega_{LO} t + \phi_{LO}(t))$. Then, the W-band signal is down-converted into an IF signal, which is expressed as

$$
\begin{aligned}
E_{IF}(t) &= \langle E_{RF}(t) \cdot E_{LO}(t) \rangle \\
&= \sqrt{P_s P_c P_{LO}} \cdot [I(t) \cdot \sin(\triangle\omega_{IF} t + \triangle\phi_{IF}(t)) + Q(t) \cdot \cos(\triangle\omega_{IF} t + \triangle\phi_{IF}(t))] \cdot \hat{e}_s \hat{e}_c \\
\triangle\omega_{IF} &= \omega_{LO} - (\omega_c - \omega_s), \quad \triangle\phi_{IF}(t) = \phi_{LO}(t) - (\phi_c(t) - \phi_s(t)).
\end{aligned}
\tag{4}
$$

The angle brackets denote low-pass filtering used for rejecting the components at $\triangle\omega + \omega_{LO}$. From the equation, it can be seen that he phase noise of the signal laser, carrier laser and LO signal are all included in $\triangle\phi_{IF}(t)$. The IF signal is then sampled and converted to digital domain, where the second stage down-conversion takes place. Assuming the sampling period of the analog-to-digital conversion (ADC) is T_s, the output signal after down-conversion and low-pass filtering can be expressed as

$$
\begin{aligned}
E_{Rx}(nT_s) &= \langle E_{IF}(nT_s) \cdot e^{j\triangle\omega_{IF} nT_s} \rangle \\
&= \frac{1}{2} \sqrt{P_s P_c P_{LO}} \cdot [I(nT_s) \cdot \sin(\triangle\phi_{IF}(nT_s)) - jI(nT_s) \cdot \cos(\triangle\phi_{IF}(nT_s)) + Q(nT_s) \\
&\quad \cdot \cos(\triangle\phi_{IF}(nT_s)) + jQ(nT_s) \cdot \sin(\triangle\phi_{IF}(nT_s))] \cdot \hat{e}_s \hat{e}_c \\
&= -\frac{1}{2} j \sqrt{P_s P_c P_{LO}} \cdot (I(nT_s) + jQ(nT_s)) \cdot e^{(j\triangle\phi_{IF}(nT_s))} \cdot \hat{e}_s \hat{e}_c.
\end{aligned}
\tag{5}
$$

It is noted that the system loss is not considered in the expressions. As shown in (5), the term $I(nT_s) + jQ(nT_s)$ is our desired QPSK signal, while the $exp(j\triangle\phi_{IF}(nT_s))$ item contains all the phase noise accumulated during the transmission, which is to be corrected during DSP demodulation [13]. The efficiency of the phase noise correction depends on the signal linewidth, which should be kept as narrow as possible by using narrow linewidth lasers for the heterodyne up-conversion [14]. It is also shown that maximum value of the signal power is achieved when the polarization states $\hat{e}_s$ and $\hat{e}_c$ are aligned.

3. Experimental Setup

Fig. 3 shows the schematic of the experimental setup. A optical carrier emitted from an external cavity laser (ECL, $\lambda_1 = 1552.0$ nm) with 100 kHz linewidth is fed into a integrated LiNbO3 I/Q modulator, where two independent 12.5 Gbaud binary data streams (pseudo-random bit sequence (PRBS) of length $2^{15} - 1$) modulate the phase of the optical carrier, resulting in a 25 Gbit/s optical baseband QPSK signal at the output of the modulator. An erbium-doped fiber amplifier (EDFA) is employed for amplification, and an optical bandpass filter (OBPF) with 0.8 nm bandwidth is used to filter the out-of-band noise. Subsequently, the optical QPSK signal is combined with an unmodulated CW optical carrier from a second ECL ($\lambda_2 = 1551.3$ nm) with 100 kHz linewidth, corresponding to a 0.7 nm difference from the central wavelength of the baseband QPSK signal.
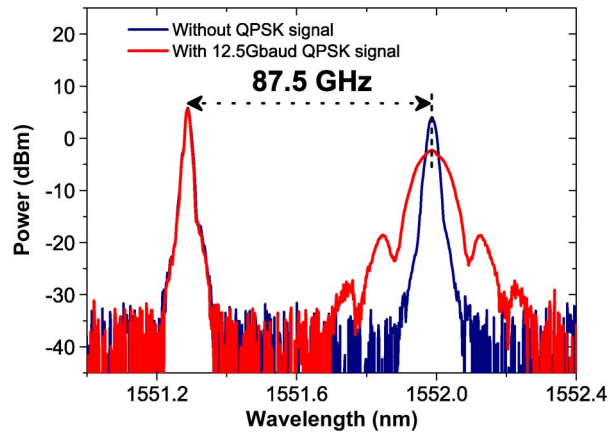
Fig. 4. Optical spectra at the input of the photodetector [point (a) in Fig. 3] with and without the QPSK data modulation.

The combined QPSK signal and the unmodulated CW carrier can be then transmitted to a RAU where they are heterodyne mixed at a 100 GHz photodetector (u^{2}t XPDV4120R). Optical transmission through 22.8 km of standard single-mode fiber (SSMF) is evaluated during the experiment. As the combined signal can be considered as a single sideband (SSB) RoF signal, the periodical RF power fading in a conventional double sideband (DSB) modulated RoF system caused by the fiber dispersion no longer exists [7]. Fig. 4 shows the optical spectra of the combined signal at point (a) in Fig. 3. The signal after the photodetection is an electrical QPSK signal at the W-band of a 25 GHz total bandwidth with the central frequency at 87.5 GHz, which is fed to a rectangular W-band horn antenna with 24 dBi gain. After wireless transmission, the W-band QPSK signal is received by a second W-band rectangular horn antenna with 25 dBi gain. The received signal is amplified by a 25 dB gain LNA (Radiometer Physics W-LNA) with a noise figure of 4.5 dB. Subsequently, an electrical down-conversion is performed at a W-band balanced mixer driven by a 74 GHz sinusoidal LO obtained after frequency doubling from a 37 GHz signal synthesizer (Rohde & Schwarz SMF 100A), and the signal located in the 75–100 GHz band is translated to a IF of 1–26 GHz with a central frequency at 13.5 GHz. The IF signal is sampled at 80 GS/s by a digital signal analyzer with 32 GHz real time bandwidth (Agilent DSAX93204A) and demodulated by offline DSP. The DSP algorithm consists of frequency down conversion, I/Q separation, synchronization, equalization, data recovery by symbol mapping, and BER tester. In the equalization module, due to the inherent constant envelop nature of the QPSK signal, a five-tap constant-modulus algorithm (CMA) pre-equalizer is first employed for blind channel equalization, followed by a carrier-phase recovery process and a post-equalization in the form of a nonlinear decision feedback equalizer (DFE). A more detailed description of the receiver can be found in [14]. We can clearly observe the performance improvement by comparing the received signal constellations with/without the CMA equalization for the 25 Gbit/s W-band QPSK signal shown in Fig. 5.

4. Experimental Results and Discussions

An optimal ratio between the carrier generating signal power P_c and the baseband QPSK signal power P_s before the combining and heterodyning is first evaluated with respect to BER performance. Fig. 6 illustrates the measured BER performance and the theoretical equivalent isotropic radiated power (EIRP) as a function of the power ratio between P_c and P_s. We can observe that the best BER performance occurs when the carrier power equals to the signal power, where the maximum signal EIRP is generated. This performance is also in accordance with that shown in (3), as the maximum RF signal power can only be obtained if P_c and P_s are equal when the combined optical power is kept constant.
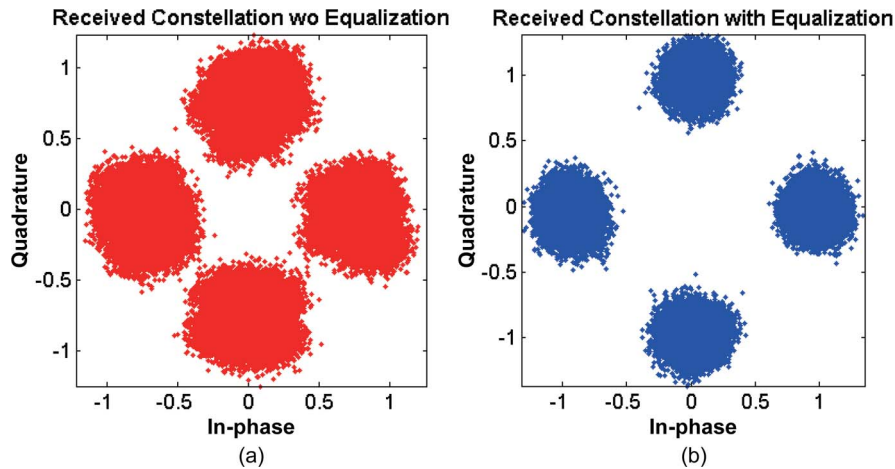
Fig. 5. Received constellations of 25 Gbit/s W-band QPSK signal after 0.5 m of air transmission. (a) Without CMA equalization. (b) With CMA equalization.
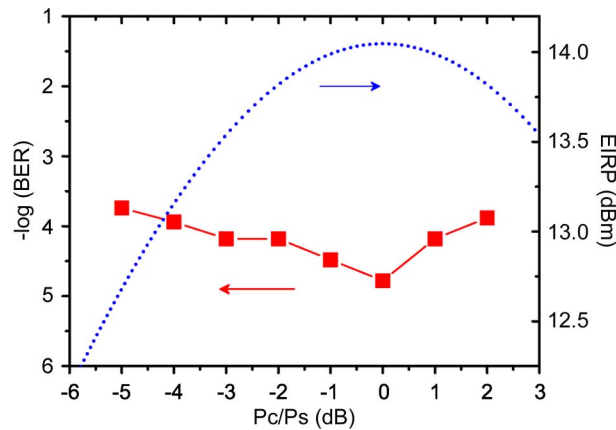

Fig. 6. Measured BER performance and simulated EIRP as a function of power ratio between the carrier generating signal and the baseband QPSK signal (P_c/P_s) with constant 1.5 dBm combined power at the PD after 1 m of wireless transmission.

After fixing the operational power ratio at the optimal value, the evaluation of the system transmission properties is performed. Fig. 7 illustrates the error-vector-magnitude (EVM) of the demodulated signal as a function of the transmitted wireless distance with the corresponding signal constellations shown in the insets. By fixing the received optical power by the PD at 1.5 dBm, it can be seen that a gradually degradation of EVM performance with the increase of the wireless transmission distance. At 50 cm, the received signal has an EVM of 26% and the clusters in the constellation are small and clearly separated, while the value becomes 53% with the distance increasing to 120 cm, and the corresponding constellation becomes disseminated, which is due to the decreased SNR at the receiver, as well as the decreased accuracy of the antenna alignment.

Fig. 8 displays the system BER performances as a function of the received optical power at the PD [point (a) in Fig. 3] with wireless distances at 1 and 2.13 m for both without optical fiber and with 22.8 km SMF transmission. It is noted that the SNR of the received IF signal is quite limited by the responsivity of the PD ($\sim$0.3 A/W at 87.5 GHz), the saturation level of the W-band LNA (-20 dBm maximum input power) and the low conversion efficiency of the broadband electrical mixer. However, considering a 7% FEC overhead can potentially be effective for BER of 2×10^{-3}, we can observe that for both the 1 m and 2.13 m wireless cases, the BERs are well below this limit.
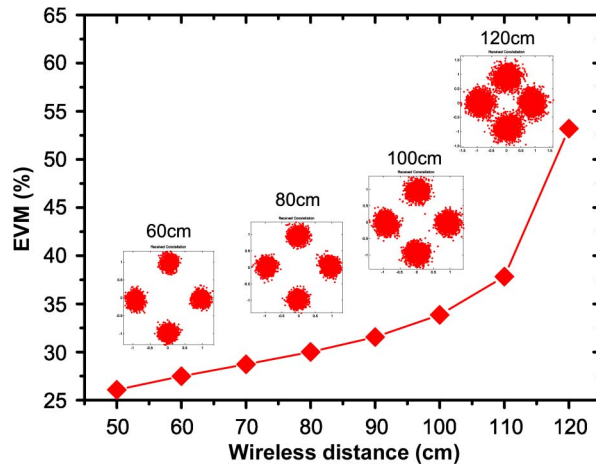
Fig. 7. EVM versus wireless distance with 1.5 dBm optical power at the PD (corresponding constellations are shown in the insets).
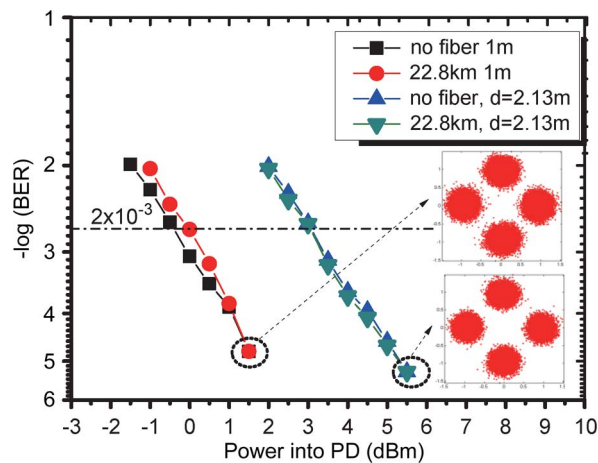

Fig. 8. BER as a function of received optical power at the PD for wireless distances at 1 and 2.13 m. (Insets: the received constellations after 1 m and 2.13 m wireless plus 22.8 km SMF transmission.)

Receiver sensitivities at the FEC limit are 0 dBm and 3 dBm for the 1 and 2 m wireless distance, respectively. It can be seen that all the measured curves are quite linear with respect to the power change, which is almost only due to change of SNR at the receiver, as the CMA equalizer can correct a certain degree of distortion introduced during the transmission. Moreover, because of the uncorrelated phase relation between the carrier and the baseband signal, the relative phase delay caused by the fiber dispersion only has effect on the baseband signal itself. It is observed that the 22.8 km SMF induces less than a 0.5 dB penalty for both cases, which confirms the possibility for integrating the proposed system with the FTTB networks.

5. Conclusion

We have demonstrated a 25 Gbit/s hybrid fiber-wireless transmission system in the W-band with 22.8 km SSMF plus up to 2.13 m of air distance. The W-band QPSK signal is generated by transparent photonic up-conversion using incoherent heterodyning between two free-running lasers. Electrical down-conversion combined with DSP receiver makes the system robust against phase noise and distortion. The RAU structure consisting of only a fast responsive PD and a transmitter

antenna is kept passive and simple to maintain its flexibility. Thus, this system may have the potential to be used in the integration of the in-building distribution networks with the fiber access networks like FTTB systems.

References

[1] T. Nagatsuma, T. Takada, H.-J. Song, K. Ajito, N. Kukutsu, and Y. Kado, "Millimeter- and THz-wave photonics towards 100-Gbit/s wireless transmission," in *Proc. 23rd Annu. Meeting IEEE Photon. Soc.*, 2010, pp. 385–386.

[2] J. Wells, "Faster than fiber: The future of multi-G/s wireless," *IEEE Microw. Mag.*, vol. 10, no. 3, pp. 104–112, May 2009.

[3] L. Deng, X. Pang, Y. Zhao, M. B. Othman, J. B. Jensen, D. Zibar, X. Yu, D. Liu, and I. Tafur Monroy, "2 × 2 MIMO-OFDM gigabit fiber-wireless access system based on polarization division multiplexed WDM-PON," *Opt. Exp.*, vol. 20, no. 4, pp. 4369–4375, Feb. 2012.

[4] C. W. Chow, F. M. Kuo, J. W. Shi, C. H. Yeh, Y. F. Wu, C. H. Wang, Y. T. Li, and C. L. Pan, "100 GHz ultra-wideband (UWB) fiber-to-the-antenna (FTTA) system for in-building and in-home networks," *Opt. Exp.*, vol. 18, no. 2, pp. 473–478, Jan. 2010.

[5] C.-T. Lin, J. Chen, W.-J. Jiang, L.-Y. Wang He, P.-T. Shih, C.-H. Ho, and S. Chi, "Ultra-high data-rate 60 GHz radio-over-fiber systems employing optical frequency multiplication and adaptive OFDM formats," presented at the Optical Fiber Commun. Conf. Expo., Nat. Fiber Optic Engineers Conf., Los Angeles, CA, 2011, Paper OThJ6.

[6] D. Zibar, A. Caballero Jambrina, X. Yu, X. Pang, A. K. Dogadaev, and I. Tafur Monroy, "Hybrid optical fibre-wireless links at the 75–110 GHz band supporting 100 Gbps transmission capacities," in *Proc MWP/APMP*, Singapore, Nov. 2011, pp. 445–449.

[7] H.-C. Chien, Y.-T. Hsueh, A. Chowdhury, J. Yu, and G.-K. Chang, "Optical millimeter-wave generation and transmission without carrier suppression for single- and multi-band wireless over fiber applications," *J. Lightw. Technol.*, vol. 28, no. 16, pp. 2230–2237, Aug. 2010.

[8] M. Weiss, A. Stohr, F. Lecoche, and B. Charbonnier, "27 Gbit/s photonic wireless 60 GHz transmission system using 16-QAM OFDM," in *Proc. Int. Topical Meeting MWP*, 2009, pp. 1–3.

[9] FCC online table of frequency allocations. [Online]. Available: www.fcc.gov/oet/spectrum/table/fcctable.pdf

[10] X. Pang, X. Yu, Y. Zhao, L. Deng, D. Zibar, and I. Tafur Monroy, "Channel measurements for an optical fiber-wireless transmission system in the 75–110 GHz band," in *Proc. Int. Topical Meeting Microw. Photon. Conf. Microw. Photon.*, 2011, pp. 21–24.

[11] Y. Zhao, L. Deng, X. Pang, X. Yu, X. Zheng, H. Zhang, and I. Tafur Monroy, "Digital predistortion of 75–110 GHz W-band frequency multiplier for fiber wireless short range access systems," *Opt. Exp.*, vol. 19, no. 26, pp. B18–B25, Dec. 2011.

[12] R. W. Ridgway, D. W. Nippa, and S. Yen, "Data transmission using differential phase-shift keying on a 92 GHz carrier," *IEEE Trans. Microw. Theory Tech.*, vol. 58, no. 11, pp. 3117–3126, Nov. 2010.

[13] D. Zibar, R. Sambaraju, A. Caballero, J. Herrera, U. Westergren, A. Walber, J. B. Jensen, J. Marti, and I. Tafur Monroy, "High-capacity wireless signal generation and demodulation in 75- to 110-GHz band employing all-optical OFDM," *IEEE Photon. Technol. Lett.*, vol. 23, no. 12, pp. 810–812, Jun. 2011.

[14] A. Caballero Jambrina, D. Zibar, R. Sambaraju, J. Marti, and I. Tafur Monroy, "High-capacity 60 GHz and 75–110 GHz band links employing all-optical OFDM generation and digital coherent detection," *J. Lightw. Technol.*, vol. 30, no. 1, pp. 147–155, Jan. 2012.

[15] Y. Zhao, X. Pang, L. Deng, X. Yu, X. Zheng, and I. Tafur Monroy, "Ultra-broadband photonic harmonic mixer based on optical comb generation," *IEEE Photon. Technol. Lett.*, vol. 24, no. 1, pp. 16–18, Jan. 2012.

[16] A. Hirata, H. Takahashi, R. Yamaguchi, T. Kosugi, K. Murata, T. Nagatsuma, N. Kukutsu, and Y. Kado, "Transmission characteristics of 120-GHz-band wireless link using radio-on-fiber technologies," *J. Lightw. Technol.*, vol. 26, no. 15, pp. 2338–2344, Aug. 2008.

[17] F.-M. Kuo, C.-B. Huang, J.-W. Shi, N.-W. Chen, H.-P. Chuang, J. E. Bowers, and C.-L. Pan, "Remotely up-converted 20-Gbit/s error-free wireless on–off-keying data transmission at W-band using an ultra-wideband photonic transmitter-mixer," *IEEE Photon. J.*, vol. 3, no. 2, pp. 209–219, Apr. 2011.

[18] A. Kanno, K. Inagaki, I. Morohashi, T. Sakamoto, T. Kuri, I. Hosako, T. Kawanishi, Y. Yoshida, and K.-I. Kitayama, "20-Gb/s QPSK W-band (75–110 GHz) wireless link in free space using radio-over-fiber technique," *IEICE Electron. Exp.*, vol. 8, no. 8, pp. 612–617, 2011.

[19] A. Kanno, K. Inagaki, I. Morohashi, T. Sakamoto, T. Kuri, I. Hosako, T. Kawanishi, Y. Yoshida, and K.-I. Kitayama, "40 Gb/s W-band (75–110 GHz) 16-QAM radio-over-fiber signal generation and its wireless transmission," *Opt. Exp.*, vol. 19, no. 26, pp. B56–B63, Dec. 2011.

[20] L. Deng, M. Beltran, X. Pang, X. Zhang, V. Arlunno, Y. Zhao, A. Caballero Jambrina, A. K. Dogadaev, X. Yu, R. Llorente, D. Liu, and I. Tafur Monroy, "Fiber wireless transmission of 8.3-Gb/s/ch QPSK-OFDM signals in 75–110-GHz band," *IEEE Photon. Technol. Lett.*, vol. 24, no. 5, pp. 383–385, Mar. 2012.

[21] X. Pang, A. Caballero Jambrina, A. Dogadaev, V. Arlunno, R. Borkowski, J. Pedersen, L. Deng, F. Karinou, F. Roubeau, D. Zibar, X. Yu, and I. Tafur Monroy, "100 Gbit/s hybrid optical fiber-wireless link in the W-band (75–110 GHz)," *Opt. Exp.*, vol. 19, no. 25, pp. 24 944–24 949, Dec. 2011.